JOURNAL OF APPLIED ELECTROCHEMISTRY 24 (1994) 411–419

Synthesis and electrochemical properties of an oxide electrode layer prepared by a new electroless plating technique

M. NAGATA, H. HOTTA, H. IWAHARA

Synthetic Crystal Research Laboratory, Nagoya University, Furo-cho, Chikusa-ku, Nagoya, 464-01, Japan

Received 5 May 1993; revised 21 September 1993

A lanthanum strontium manganese thin oxide layer was plated on yttria stabilized zirconia by oxidizing the lanthanum strontium manganese ions with hydrogen peroxide as the oxidant. The plated oxide layer was firmly adherent to the substrate, and its morphology was finely porous. The crystal phase of the oxide was determined by XRD to be a perovskite-type. The mechanism for the oxide layer formation by an oxide electroless plating was studied by means of ESCA. As a cathode of solid oxide fuel cell (SOFC), the electrode characteristics of an oxide plated in this way were measured by the current interruption method at 1000° C. The cathodic overpotential of this electrode was less than 40 mV at 1 A cm^{-2}. This small overvoltage was considered to be based on an effective large electrode reaction area.

1. Introduction

Recently, the high temperature solid oxide fuel cell (SOFC) has received much attention as an effective and clean energy converter, and many studies have been made on its electrolyte, electrode and electric generation systems. As a solid electrolyte, yttria-stabilized zirconia (YSZ) is the most promising from the standpoint of chemical stability, although its conductivity is relatively small (0.1 S cm^{-1} at 1000° C). As a practical cathode material for SOFC, strontium-doped lanthanum manganese oxide ($La_{1-x}Sr_xMnO_3$: LSM) is the most useful in terms of the electrode characteristics and cost.

Two well known methods of attaching the LSM to the YSZ electrolyte are plasma-spraying and sputtering [1–3]. Because these are gas phase processing methods, significantly good contact conditions between the electrode and the electrolyte can be obtained; a thin and homogeneous electrode layer can be produced on the electrolyte. But these methods need complex devices and have expensive fabrication costs. As a simplified method for attaching the electrode, a powder smearing and a screen printing method are commonly used. In that case, a fine LSM powder must be prepared to obtain good electrode characteristics. To make a fine LSM powder, several methods have been developed: for example a ceramic method [4–6], a drip pyrolysis method [7], a freeze-drying method [8], a coprecipitation method [9], and a sol–gel method [10]. However, it is difficult to obtain good contact conditions between the electrode and the electrolyte because both the smearing and the screen printing methods are solid phase methods. If fine LSM could be attached firmly to the electrolyte using a simplified method, it might contribute to the practical fabrication of SOFC.

To fabricate the LSM layer on the YSZ substrate, an electroless plating method was investigated. The electrochemical properties of metal electrodes (Pt and Ni) attached by such a method have been reported [11, 12]. In these studies, plated metal electrodes showed better electrode characteristics as compared with smeared electrodes. The electroless plating of metals is a well-known method for preparing a thin metal layer on a ceramic substrate. In this method, a reductant reagent (e.g. hydrazine) is used to reduce metal ions to metal.

$$M^{n+} \xrightarrow{\text{reductant}} M_{\text{metal}}$$

On the other hand, electroless plating of an oxide is achieved by oxidizing metal ions with an oxidant (e.g. hydrogen peroxide, sodium nitrate, etc.).

$$M^{n+} \xrightarrow{\text{oxidant}} MO_x$$

As a method for preparing an oxide on the non-conductive substrate using this reaction, ferrite coating by a liquid phase oxidation method has been reported [13–16]. Several kinds of ferrite were produced by oxidizing ferrous and other ions on the substrate (e.g. silica glass). The present authors have also reported on an electroless plating of manganese oxide [17]. The plated manganese oxide had a Mn_2O_3 (cubic, bixbyite-c) crystal phase when left in its original state, and a chemical bond between the plated oxide and YSZ substrate was considered to exist because the adhesion was very high.

In this study an attempt was made to plate a controlled composition LSM oxide layer directly onto the YSZ substrate using the oxide electroless plating

0021-891X

method. The crystallography of the plated oxides were studied. The microstructure and the nature of the bond between the plated oxide and the YSZ substrate, and the formation mechanism of the oxide layer was discussed. Finally, electrochemical cells were constructed to study the properties of the plated oxide as cathode in a SOFC.

2. Experimental details

2.1. *Formation of the La(Sr)MnO_3 layer and its analysis*

As the sources for lanthanum, strontium and manganese, lanthanum oxide (La_2O_3), strontium nitrate ($Sr(NO_3)_2$) and manganese nitrate ($Mn(NO_3)_2 \cdot 6H_2O$) were used, respectively. La_2O_3 was dissolved in concentrated nitric acid and the resultant nitrate was mixed with a strontium and manganese nitrate solution. The mole fraction of $La^{3+}:Sr^{2+}:Mn^{2+}$ in the starting solution was changed to $(La^{3+}+Sr^{2+}):Mn^{2+}=1:r$, and the ratio of $La^{3+}:Sr^{2+}$ in $(La^{3+}+Sr^{2+})$ was changed. The concentration of total components in the starting solution was 0.01 M. The solution was pumped out by a micro tube pump onto the substrate. It was oxidized with 20% hydrogen peroxide solution in which concentrated ammonia water was added to control pH. The hydrogen peroxide solution was also pumped out by the micro tube pump onto the substrate, as reported in [17]. The flow rates of both solutions were 1.0 ml min^{-1}. Yttria stabilized zirconia ceramic, $(ZrO_2)_{0.92}(Y_2O_3)_{0.08}$, (made by Tosoh, TZ-8Y powder) was used as a substrate after being ground with abrasive paper (no. 600). Composition of the plated oxide was determined by ICP after the oxide was dissolved in a dilute hydrogen chloride solution. The microstructure of the plated oxide layer was observed by SEM, and the element distribution over the oxide was made by EPMA. The crystal phase was determined by X-ray diffraction (XRD). The mechanism for an oxide electroless plating was analyzed using the data obtained from the above measurements. The chemical bond between the plated oxide and YSZ substrate was studied by observing the oxide layer–substrate interface using ESCA (VG Escalab Mk II MgK_α).

2.2. *Electrochemical measurement*

Electrochemical cells were constructed with YSZ discs of diameter 14 mm, thickness 0.5 mm, and area 0.5 cm^2. Details of the test cell are described elsewhere [11]. Electrochemical properties of SOFC as a cathode were measured at 1000° C by the current interruption method with a pulse width of 0.001 s and a pulse period of 0.020 s (Nikko Keisoku current pulse generator NCPG-101). Also complex impedance measurements were made with a frequency range of 100 kHZ–1 Hz (Solartron 1255 HF frequency analyser and SI 1286 electrochemical interface). Hydrogen and air were introduced to the anode and cathode of the SOFC, respectively. Ni–YSZ cermet (nickel content 40 vol %) was used as an anode.

3. Results and discussion

3.1. *Plated oxide layer composition*

The dependence of the mole fraction of each component ($La^{3+}:Sr^{2+}:Mn^{2+}$) in the starting solution on the chemical composition of the prepared oxide was studied. The $La^{3+}:Sr^{2+}:Mn^{2+}$ ratio was varied as follows: $1:0:r$, $0.75:0.25:r$, $0.5:0.5:r$, $0.25:0.75:r$ and $0:1:r$ (here the Mn^{2+} ratio r varied from 0.1 to 1.0). The composition of the prepared oxide, (La + Sr)/Mn, is plotted against the ratio of the starting solution ratio in Fig. 1(a)–(e). Since lanthanum strontium manganese oxide is a perovskite-type oxide (indicated as ABO_3: A and B are cations), the plated oxide takes a perovskite-type crystal phase when (La + Sr)/Mn is 1 (indicated by a broken line in Fig. 1). In an oxide plating of lanthanum and manganese only, the lanthanum content in the plated oxide simply decreases with increase in Mn^{2+} content in the starting solution, as shown in Fig. 1(a). On the other hand, maximum strontium content was observed in plating of strontium and manganese only, as shown in Fig. 1(e). Because of the two different plating characteristics observed in the La–Mn and Sr–Mn systems, the tendency of composition variation of the plated oxide may be changed according to the $La^{3+}:Sr^{2+}:Mn^{2+}$ ratio in the starting solution, as shown in Fig. 1(b)–(d). In this oxide formation, manganese oxide is preferentially plated on the substrate, and lanthanum and strontium oxide is likely held by manganese oxide, i.e. as an anchoring effect [17]. Thus, when the Mn^{2+} ratio r in the starting solution is below 0.25, the oxide cannot be plated.

To study the relation between the mole fractions of each component in the starting solution and the prepared oxide when the Mn^{2+} ratio r in the starting solution is constant, the data shown in Fig. 1 were replotted against the ratio $Sr^{2+}:La^{3+}$ when r is 0.375, 0.500, 0.625 and 0.750, respectively, as shown in Fig. 2. From the reactivity of the electrode with the electrolyte at high temperature (~1000° C) [18] and from the characteristics as a SOFC cathode, the best composition of $La_{1-x}Sr_xMnO_3$ is presently considered to be $(La_{0.7}Sr_{0.3})_{0.95}MnO_3$. (This point is still under investigation.) This composition could be obtained when the ratio of $La^{3+}:Sr^{2+}:Mn^{2+}$ was 0.4 : 0.6 : 0.5 as shown in Fig. 2(b). Of course, an oxide of different composition could be prepared (e.g. $La_{0.8}Sr_{0.2}MnO_3$, $La_{0.7}Sr_{0.3}MnO_3$, etc.) by changing the $La^{3+}:Sr^{2+}:Mn^{2+}$ ratio of the starting solution.

3.2. *Crystallography*

Typical XRD patterns of the plated oxide layers are

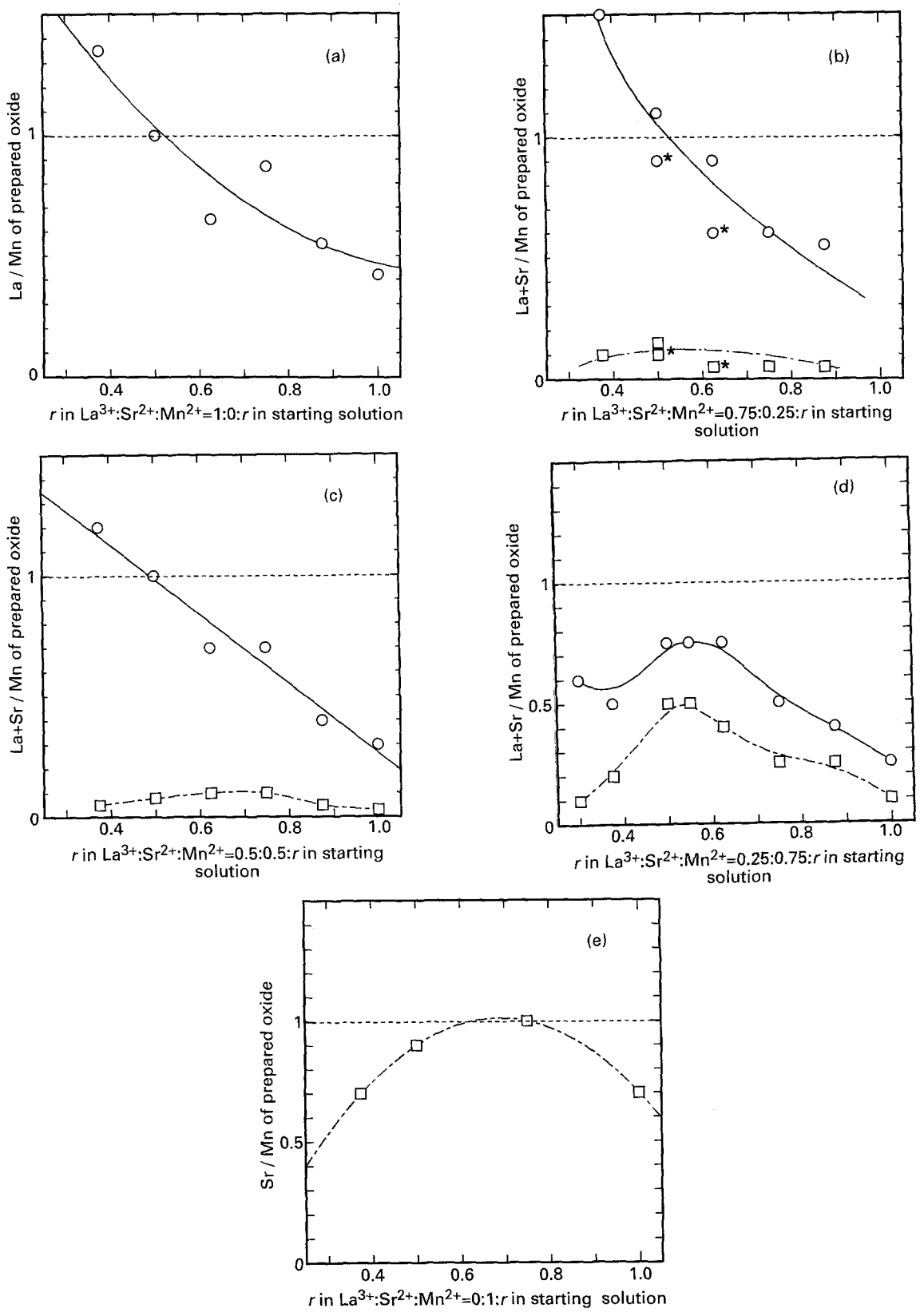

Fig. 1. Composition dependence of the prepared oxide on the starting solution ratio. Composition of the plated oxide is plotted against Mn^{2+} ratio r in starting solution. (○) La + Sr, (□) Sr. *means set of samples.

shown in Fig. 3. The as-prepared oxide appeared to be amorphous and only diffraction lines of YSZ substrate were observed (data not shown). In the pattern of the specimen (La/Sr/Mn = 0.53/0.24/1 from ICP) fired at 1000° C, however, peaks of a perovskite-type oxide ($La_{0.8}Sr_{0.2}MnO_3$ in JCPDS) were observed with the peaks of substrate (the peaks of YSZ substrate have been removed from Fig. 3 to make the oxide peaks clear). Although the A site in ABO_3 (La and Sr in $La(Sr)MnO_3$) is lacking in the composition of the plated oxide, no second phase (e.g. Mn_2O_3) was observed. When the lanthanum content in the prepared oxide was high (for example, La/Mn = 1.1), the diffraction lines of La_2O_3 were observed in addition to the peaks of LSM, as shown in Fig. 3(a). On the other hand, the peak of strontium

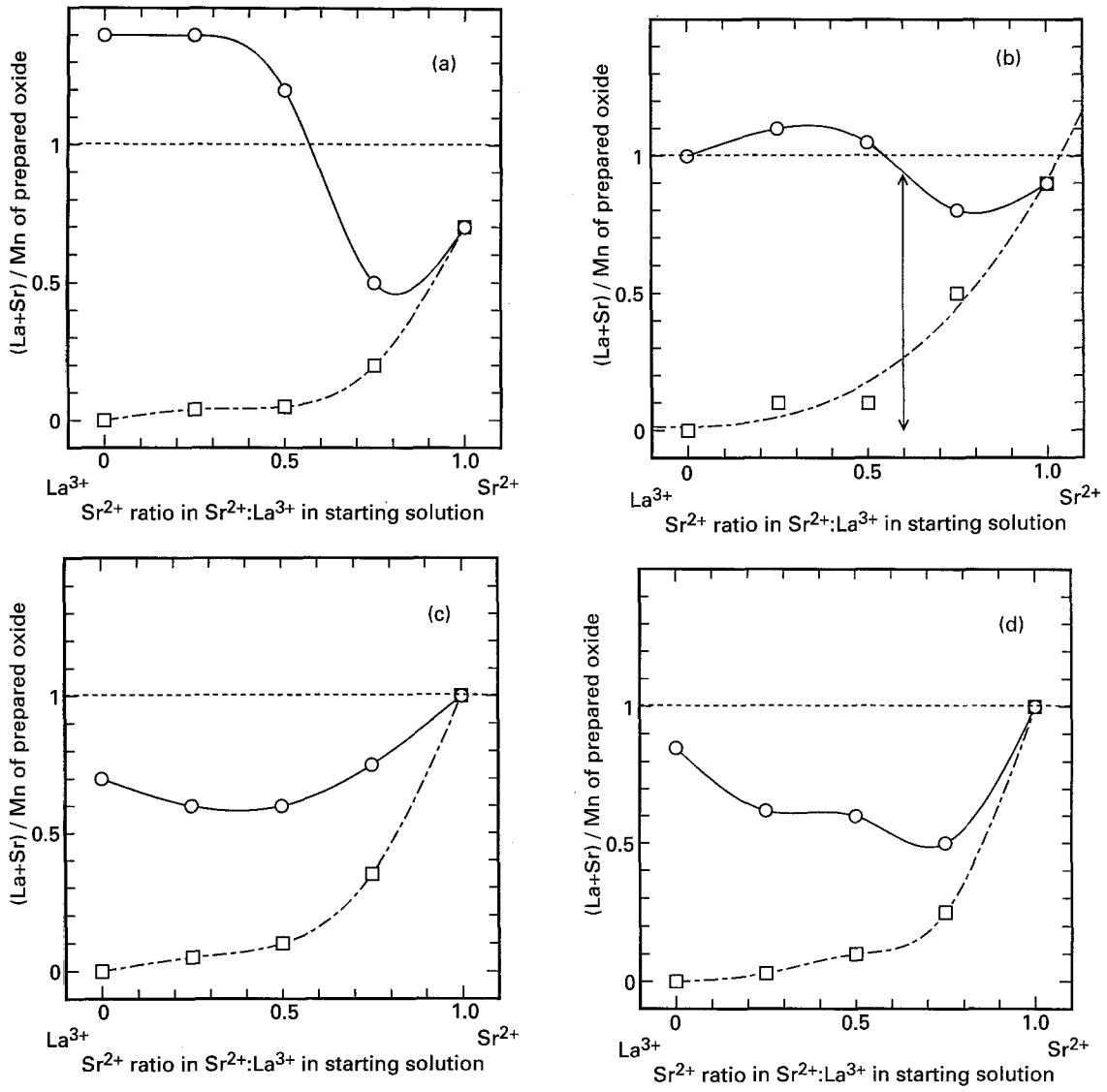

Fig. 2. Composition dependence of the prepared oxide on the starting solution ratio. Composition of the plated oxide is plotted against Sr^{2+} ratio of Sr^{2+} : La^{3+} in starting solution. Mn^{2+} ratio r in starting solution is (a) 0.375, (b) 0.500, (c) 0.625 and (d) 0.750. The composition of the starting solution that will make an oxide layer with the ideal composition $(La_{0.7}Sr_{0.3})_{0.95}MnO_3$ is indicated by an arrow in (b). (○) La + Sr, (□) Sr.

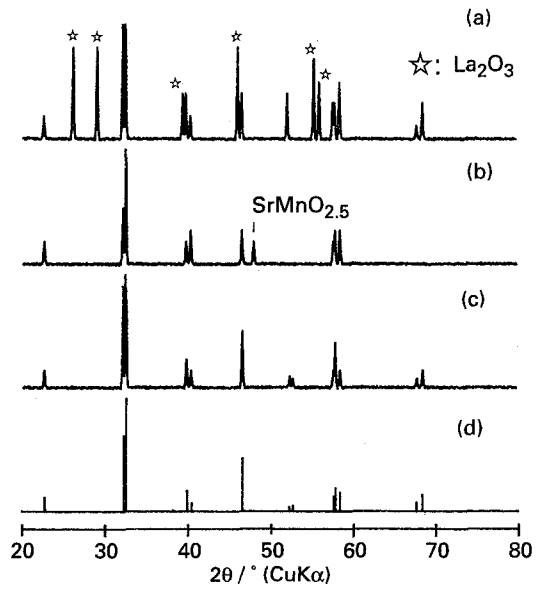

Fig. 3. XRD patterns of the plated oxide layer in which (a) La content is high; (b) Sr content is high; and (c) La : Sr : Mn in the plated oxide is 0.53 : 0.24 : 1. (d) shows $La_{0.8}Sr_{0.2}MnO_3$ (JCPDS).

manganese oxide ($SrMnO_{2.5}$) was observed when the strontium content in the plated oxide was high (Fig. 3(b)).

3.3. *SEM observation and element distribution over the plated oxide*

SEM pictures of an as-prepared oxide layer (prepared as $(La_{0.7}Sr_{0.3})_{0.95}MnO_3$) on YSZ are shown in Fig. 4(a) and (b). Fine particles were plated onto the YSZ substrate and the thickness of the oxide layer was about 5 μm. The oxide layer was porous and somewhat rough, but, significantly good contact with the electrolyte was observed. In addition, the adhesion strength of the oxide layer to the electrolyte was high.

Pictures of the oxide layers after firing at 1000° C for 5 h are shown in Fig. 4(c) and (d). Fine particles (<0.5 μm) were observed in the plated oxide, and this morphology was different from the screen-printed LSM which was fired at 1200° C in air for 2 h (Fig. 4(e)). Here the screen-printed LSM has micro-

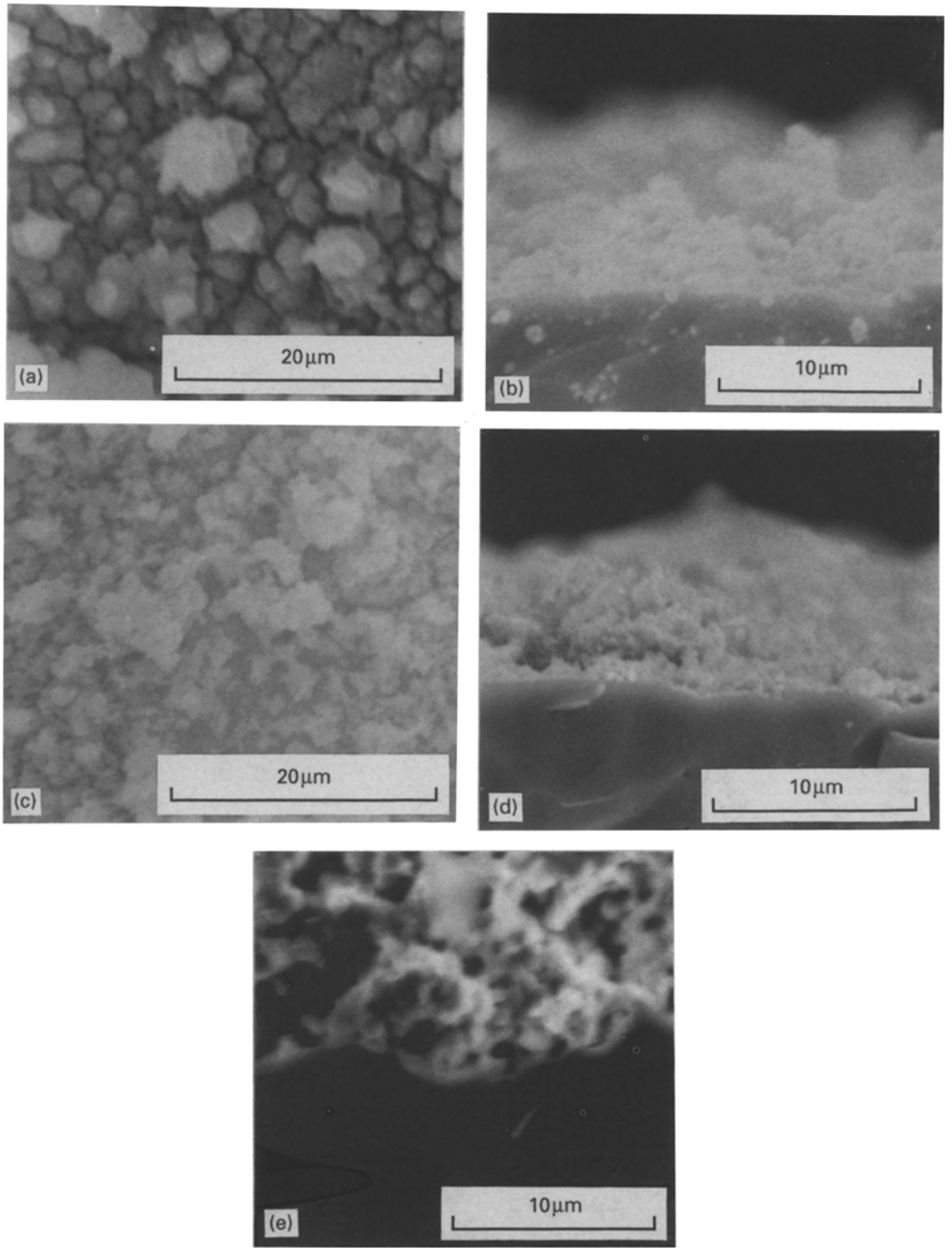

Fig. 4. SEM images of oxide layers: (a) surface and (b) fractured surface of as-prepared plated oxide layer, (c) surface and (d) fractured surface of plated oxide fired at 1000° C in air; (e) fractured surface of screen-printed $La_{0.6}Sr_{0.4}MnO_3$ fired at 1200° C in air. In (b), (d) and (e) the lower sections are YSZ.

meter order particles. The so-called three-phase reaction area (gas/electrode/electrolyte) of the plated oxide electrode appears to be larger than that of the screen printed LSM. Lanthanum, strontium and manganese EPMA maps (Fig. 4(c)) are shown in Fig. 5. These maps show that lanthanum, strontium and manganese distribute homogeneously over the oxide membrane.

3.4. *Oxide layer formation mechanism*

3.4.1. Mn_2O_3 plating. As reported previously [17], the as-prepared plated oxide shows an XRD pattern of Mn_2O_3 when only manganese is used as a metal ion source. (This is completely different from La(Sr)MnO_3 plating in which the plated oxide is

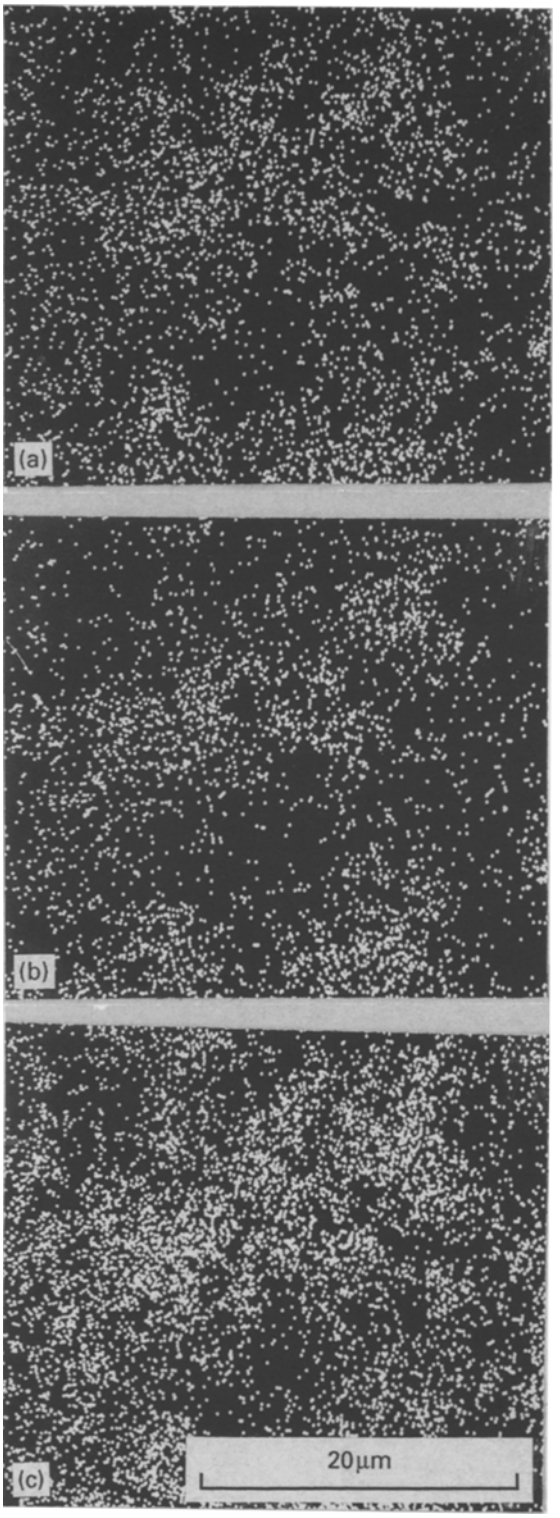

Fig. 5. EPMA maps of the surface of the fired plated oxide layer (Fig. 5(c)): (a) La map, (b) Sr map, (c) Mn map.

considered to be amorphous when it is as-prepared.) The adhesion strength of this manganese oxide to the substrate was measured by tensile testing. The plated Mn_2O_3 was attached to an iron rod with glue (Sumitomo 3M Scotch Weld SW-2214) and the YSZ substrate was also attached to the rod, as shown in Fig. 6. The tensile test was made by stretching both rods (Auto Graph was used). Since the adhesion strength of the plated oxide to the substrate was higher than that of the glue itself, the oxide layer could not be peeled off; i.e. the interface between the

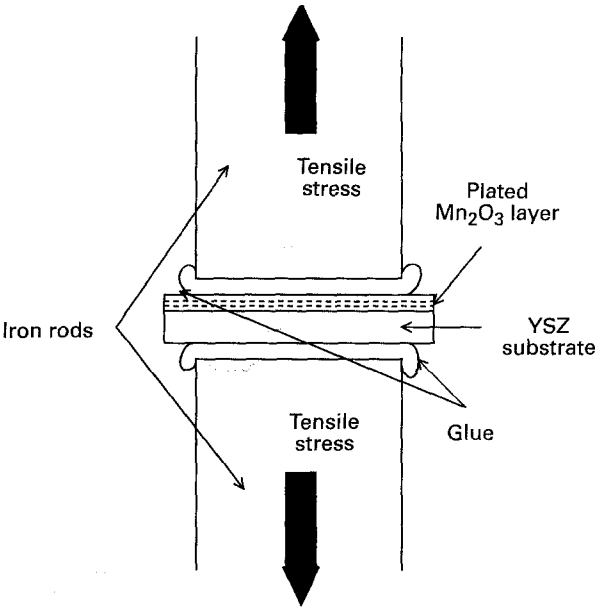

Fig. 6. Schematic diagram of the tensile stress test. The diameters of the iron rod and YSZ substrate were 11 mm and 14 mm, respectively.

rod and the oxide or the rod and substrate was peeled off. From this observation, the adhesion strength of the plated Mn_2O_3 to the YSZ substrate was estimated to be higher than 500 kg cm^{-2}. An SEM picture of an interface between Mn_2O_3 and the YSZ substrate is shown in Fig. 7, where significantly good contact can be observed. (The oxide here was dense.)

From this high adhesion strength, the possibility of a chemical bond of manganese and YSZ at the interface was considered. To prove the existence of such a chemical bond between Mn_2O_3 and YSZ, a surface analysis at the Mn_2O_3–YSZ interface was made by ESCA. The peaks of Mn2p are shown in Fig. 8. (The spectra (a), (b) and (c) were measured on different samples, so the intensities could not be easily compared.) By contrast with the peaks of the oxide surface (spectrum (a)), clear satellite peaks were observed at the plane that was considered to be an

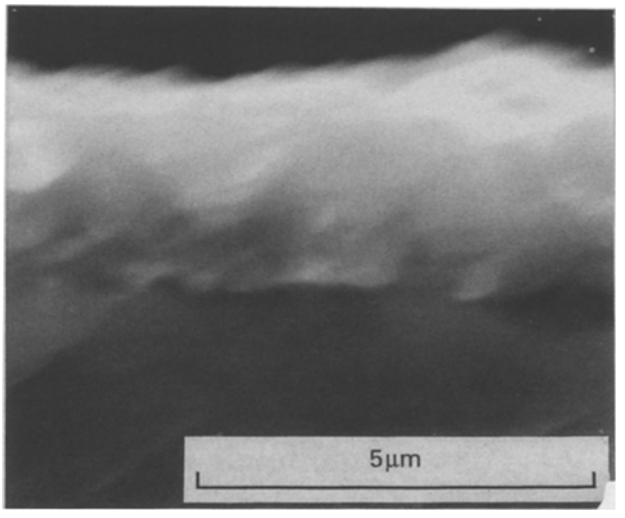

Fig. 7. SEM image of the as-prepared plated manganese oxide on YSZ. The crystal phase of the plated oxide was Mn_2O_3.

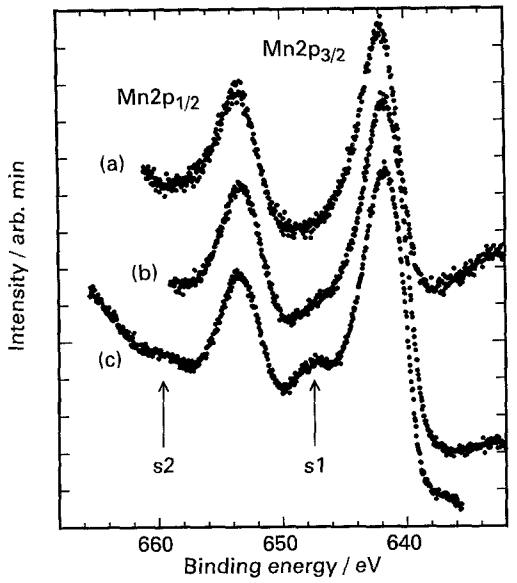

Fig. 8. The spectra of Mn2p measured by ESCA: (a) surface of the plated oxide (Mn_2O_3) without argon sputtering; (b) surface of the plated oxide after argon sputtered; (c) interface between the plated oxide and YSZ substrate. s1 is a satellite peak of $Mn2p_{3/2}$ and s2 of $Mn2p_{1/2}$.

interface (spectrum (c)). The interface plane was revealed by etching the oxide (argon sputtering). Here, argon sputtering seems to affect the appearance of the satellite peaks, as shown in spectrum (b), where the oxide surface was sputtered under the same conditions as when the sample of spectrum (c) was measured. However, when comparing the intensity of $Mn2p_{3/2}$ peaks, the intensity of the satellite peak at 647 eV in the spectrum (c) was much higher than that in the spectrum (b) in Fig. 8 (see Table 1). Thus, the authors determined that spectrum (c) shows the interface of the Mn_2O_3 layer and the YSZ substrate. The satellite peaks were considered to be doublets of $Mn2p_{3/2}$ and $Mn2p_{1/2}$ [19], respectively, because of the chemical shift and the ratio of intensities seen in Table 1: The difference in the binding energy of satellites was equal to that of $Mn2p_{3/2}$ and $Mn2p_{1/2}$ (this was about 12 eV), and the ratio of intensities [(satellite of $Mn2p_{3/2}$)/$Mn2p_{3/2}$ and (satellite of $Mn2p_{1/2}$)/$Mn2p_{1/2}$] was 0.153 and 0.088. (These should be the same, but the intensity of the satellite peak of $Mn2p_{1/2}$ was considered to be less than the real value because of the difficulty of peak fitting: the background became increasingly high over 660 eV). This indicates that the valence or the

Table 1. Binding energies, intensities and widths of Mn2p peaks in Fig. 8(b) and (c) after the peaks were fitted

		$Mn2p_{3/2}$	*Satellite*	$Mn2p_{1/2}$	*Satellite*
(b)	Binding energy/eV	641.63	647.36	653.17	
	Intensity	8023	312	3342	
	Width	3.73	2.00	3.40	
(c)	Binding energy/eV	641.39	647.64	653.43	659.89
	Intensity	8037	1230	3030	267
	Width	3.59	3.05	3.38	2.90

Charge-ups were revised by $Au4f_{7/2}$ 83.7 eV. Peaks were fitted by the gauss value of 80% in all cases.

bonding conditions of manganese at the interface are different from those in the Mn_2O_3 layer. The details remain unclear, but the existence of a chemical bond between Mn_2O_3 and the YSZ substrate is indicated, and the presence of such a bond is the likely reason for the high adhesion strength of the Mn_2O_3 layer to the YSZ substrate.

3.4.2. La(Sr)MnO_3 plating. Although an attempt was made to plate lanthanum and strontium oxide individually, the plating was unsuccessful (only some soft deposits were observed on the substrate). In the case of lanthanum oxide plating, the deposits were La_2O_3 and $La(OH)_3$; in the case of strontium oxide plating, they were SrO and SrO_2. (Deposits were characterized by XRD.) Since manganese oxide could be prepared with a high adhesion strength, the formation of La(Sr)MnO_3 was thought to have been achieved by an anchoring effect: i.e. manganese oxide attaches to the substrate preferentially and lanthanum and strontium oxide (and/or hydroxide) are caught by the manganese oxide when the oxide layer is formed. In addition, bubbles, arising from the decomposition of hydrogen peroxide, remove lanthanum and strontium oxide during the plating reaction [17]. The different tendencies of prepared oxide composition depending on the starting solution (shown in Fig. 1(b)–(d)) may be caused by the different characteristics of lanthanum and strontium deposits (e.g. surface area, mass of their respective particles, and affinity to manganese oxide, etc.). Due to a mechanism of this kind, the adhesion strength of the La(Sr)MnO_3 layer is considered to be less than that of the Mn_2O_3 layer.

3.5. *Electrochemical properties of the plated oxide as a SOFC cathode*

The electrode characteristics of the plated oxide layer as a SOFC cathode were studied by constructing an electrochemical cell at 1000° C in air. The electrode characteristics of the plated LSM were compared with the characteristics of the screen-printed $La_{0.6}Sr_{0.4}MnO_3$, which was prepared by a drip

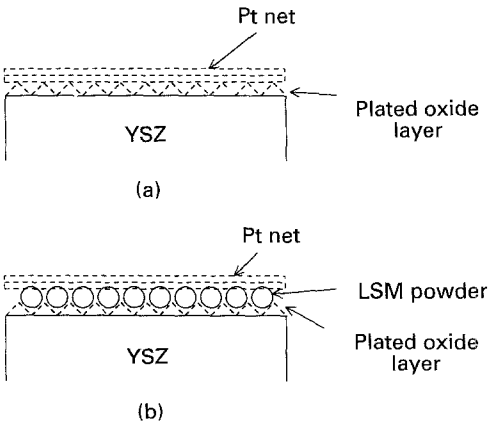

Fig. 9. Schematic illustration of current collector conditions: (a) only a platinum mesh was used as a current collector; (b) LSM powder was smeared on the plated oxide layer as a current collector.

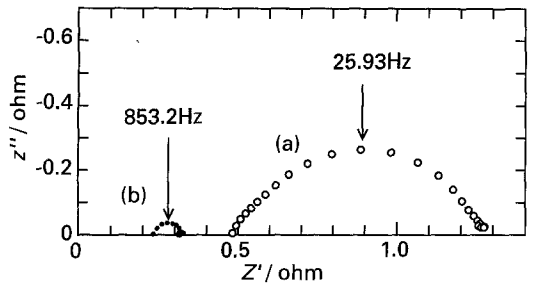

Fig. 10. Typical Cole–Cole plots measured at 1000° C in air: (a) screen-printed $La_{0.6}Sr_{0.4}MnO_3$; (b) plated oxide on which $La_{0.6}Sr_{0.4}MnO_3$ powder was smeared.

pyrolysis method. (It was fired at 1200° C for 2 h in air after screen printing, the screen was 200 mesh and the diameter of the lines were 47 μm.) Since the plated oxide layers were thin (5–10 μm), $La_{0.6}Sr_{0.4}MnO_3$ powder prepared by the drip pyrolysis method was smeared on the layers to help the electric conduction in the planar direction, as illustrated in Fig. 9(b). Fig. 10(a) and (b) show the typical Cole–Cole plots of screen-printed $La_{0.6}Sr_{0.4}MnO_3$ and the plated oxide layer on which the $La_{0.6}Sr_{0.4}MnO_3$ was smeared. (In this experiment, Cole–Cole plots were measured between the cathode and reference electrode.) The diameter of the semicircle of the plated LSM is much smaller than that of the screen-printed LSM. This indicates that the reaction resistance of the plated LSM is smaller than that of the screen-printed LSM [20].

Cathodic overvoltages measured by the current interruption method are shown in Fig. 11. When the plated oxide layer (the composition of La/Sr/Mn was 0.53/0.24/1, derived from ICP) was used as a cathode with only a platinum net current collector as shown in Fig. 9(a), a small overvoltage was observed, but the ohmic drop was large in this case (twice the value calculated from the conductivity of YSZ and the cell constant). This indicates the resistance of the oxide layer in the planar direction is high.

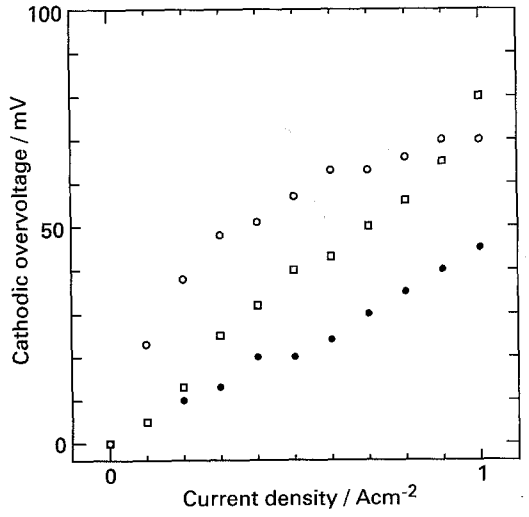

Fig. 11. Cathodic overvoltages measured by the current interruption method at 1000° C in air: (○) plated oxide with only a platinum mesh current collector; (□) screen-printed $La_{0.6}Sr_{0.4}MnO_3$; (●) plated oxide layer on which the $La_{0.6}Sr_{0.4}MnO_3$ powder was smeared.

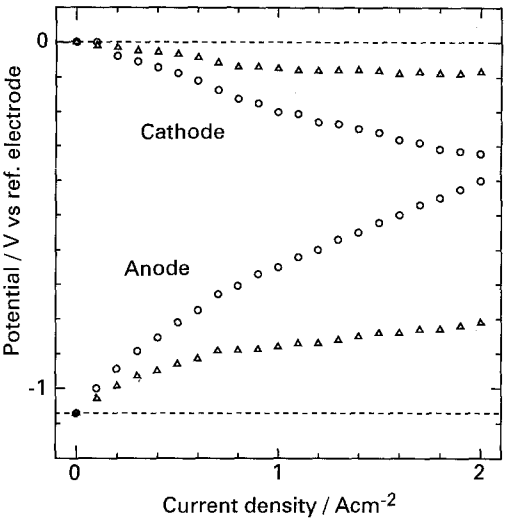

Fig. 12. Polarization curves of hydrogen–air fuel cell at 1000° C. H_2Ni cermet | YSZ | LSM air. (○) Total potential. (△) IR free.

This is due to the small thickness of the layer (about 5 μm) and low conductivity of the LSM, which is three orders lower than that of platinum. When the $La_{0.6}Sr_{0.4}MnO_3$ powder was smeared on the plated oxide layer (prepared as $(La_{0.7}Sr_{0.3})_{0.95}MnO_3$) to help electrical conduction in the planar direction (as shown in Fig. 9(b)), a small overvoltage was observed (40 mV at 1 A cm^{-2}) without excess ohmic resistance. This value is smaller than that of screen-printed $La_{0.6}Sr_{0.4}MnO_3$, which shows the best electrode characteristics but is not a practical composition.

Finally, a hydrogen–air fuel cell was constructed with an electrolyte of 0.37 mm thickness. The cathode was a plated LSM on which $La_{0.6}Sr_{0.4}MnO_3$ was smeared and the anode was the usual Ni–YSZ cermet (Ni : YSZ, 40 : 60 vol %) fired at 1400° C. Figure 12 shows the polarization curves during discharge. The cathodic overvoltage was sufficiently small at high current density (<100 mV at 2 A cm^{-2}), although the anodic overvoltage was large, probably due to less than optimal experimental conditions. Figure 13 shows the output power density of this cell, in which a maximum power of 0.45 W cm^{-2} was obtained.

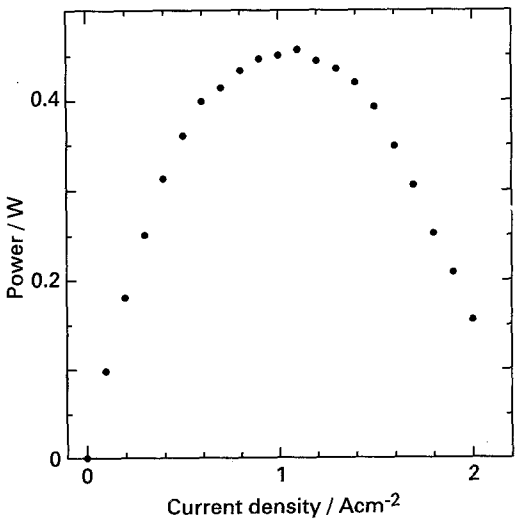

Fig. 13. Power density of hydrogen–air fuel cell at 1000° C.

4. Conclusion

Lanthanum strontium manganese oxide could be plated on the YSZ substrate by the oxide electroless plating method. The adhesion strength of the manganese oxide was significantly high ($>500\,kg\,cm^{-2}$), and a chemical bond between manganese and the YSZ substrate was investigated by using ESCA. The formation of the $La(Sr)MnO_3$ layer could be achieved by the anchoring of lanthanum and strontium deposits with manganese oxide. The plated LSM layer showed a small cathodic overvoltage when it was used as a precoating material for the cathode. Oxide electroless plating is a promising technique for SOFC fabrication.

Acknowledgements

The authors wish to thank Dr M. Yanagisawa, Y. Yamamoto and I. Satoh of the Japan Fine Ceramics Center for the use of ICP and Dr N. Shibata and F. Kawashima also of the JFCC for their help with the ESCA.

References

[1] R. Okiai, S. Yoshida, I. Kaji, M. Hasegawa, H. Yamanouchi and M. Nagata, *Proc. SOFC Nagoya* **115** (1989).
[2] O. Yamamoto, Y. Takeda, R. Kanno and M. Noda, *Solid State Ionics* **22** (1987) 241.
[3] Y. Takeda, R. Kanno, M. Noda, Y. Tomita and O. Yamamoto, *J. Electrochem. Soc.* **134** (1987) 2656.
[4] M. Kertesz, I. Riess and D. S. Tannhauser, *J. Solid State Chem.* **42** (1982) 125.
[5] A. Hammouche, E. Siebert and A. Hammou, *Mat. Res. Bull.* **24** (1989) 367.
[6] A. Hammouche, E. Siebert, A. Hammou and M. Kleitz, *J. Electrochem. Soc.* **138** (1991) 1212.
[7] J. Mizusaki, H. Tagawa, K. Naraya and T. Sasamoto, *Solid State Ionics* **49** (1991) 111.
[8] J. Mizusaki, Y. Mima, S. Yamauchi, K. Fueki and H. Tagawa, *J. Solid State Chem.* **80** (1989) 102.
[9] J. Mizusaki, T. Sasamoto, W. R. Cannon and H. K. Brown, *J. Am. Ceram. Soc.* **66** (1983) 247.
[10] S. Bilger, E. Syskakis, A. Naoumidis and H. Nickel, *J. Am. Ceram. Soc.* **75** (1992) 964.
[11] M. Nagata, T. Esaka and H. Iwahara, *Denkikagaku* **59** (1991) 707.
[12] *idem, ibid.* **60** (1992) 792.
[13] M. Abe and Y. Tamaura, *Jpn. J. Appl. Phys.* **22** (1983) 511.
[14] *idem, J. Appl. Phys.* **55** (1984) 2614.
[15] M. Abe, Y. Tanno and Y. Tamaura, *J. Appl. Phys.* **57** (1985) 3795.
[16] Y. Tamaura, Y. Tanno and M. Abe, *Bull. Chem. Soc. Jpn.* **58** (1985) 1500.
[17] M. Nagata and H. Iwahara, *Mat. Res. Bull.* **28** (1993) 255.
[18] J. A. M. van Roomalen and E. H. P. Cordfunke, *Solid State Ionics* **52** (1992).
[19] S. P. Kowalczyk, L. Ley, R. A. Pollak, F. R. McFeely and D. A. Shirly, *Phys. Rev. B* 7(8) (1973) 4009.
[20] J. Mizusaki, H. Tagawa, K. Tsuneyoshi and A. Sawata, *J. Electrochem. Soc.* **138** (1991) 1867.